SLAC-PUB-3924
SCIPP 86/57
UH-511-585-86
April 1986
(I/E)

TEST BEAM RESULTS FOR SILICON MICROSTRIP DETECTORS WITH VLSI READ-OUT*

CHRIS ADOLPHSEN, ALAN LITKE,
ANDREAS SCHWARZ, AND MICHAL TURALA†

Santa Cruz Institute for Particle Physics
University of California, Santa Cruz, CA 95064

VERA LÜTH

Stanford Linear Accelerator Center
Stanford University, Stanford, California, 94305

ALAN BREAKSTONE AND SHERWOOD PARKER

University of Hawaii, Honolulu, HI 96822

ABSTRACT

A telescope consisting of three silicon microstrip detectors has been tested in a high energy positron beam at SLAC. Each detector has strips with 25 micron pitch and is read out by two 128-channel NMOS integrated circuits ("Microplex"). Results on the signal-to-noise ratio, spatial resolution, and two-track separation are given.

Presented at the Fourth European Symposium on
Semiconductor Detectors, Munich, F.R. Germany, March 3-5, 1986

---

* Work supported by the Department of Energy, Contracts DE-AC03-76SF00515, DE-AA03-76SF00034, and DE-AC03-83ER-40103

† Visitor from the Institute of Nuclear Physics, Krakow, Poland

1. Introduction

Over the last few years silicon microstrip detectors have been developed and successfully employed as vertex detectors in fixed target experiments [1]. Recently, several groups have proposed to use microstrip detectors in colliding beam experiments [2]. In particular, we are developing a vertex detector for the MARK II experiment at the SLAC Linear Collider to study short-lived particles produced in the decay of the Z^0 [3].

This silicon strip vertex detector will consist of three layers with a total of over eighteen thousand detecting strips. As the outer radius is less than 4 cm, it is clearly impractical to consider using conventional readout electronics. Instead, we plan to use the Microplex integrated circuit [4-6] which provides 128 channels of charge-sensitive amplifiers with multiplexed analog output on a single chip 4.7×6.4 mm^2 in area.

As operating experience with silicon strip detectors equipped with Microplex chips has so far been limited (see references 5 and 6 for previous results), we assembled a telescope consisting of three such detectors. In this paper, we report on the results from a beam test performed at the Stanford Linear Accelerator Center.

2. The Telescope

Table 1 summarizes the properties of the three silicon detectors that make up the telescope. Each detector [7] has diode strips with a pitch of 25 μm. We note that detector B has a wide implant of 17 μm and that detector C, due to a large leakage current, was operated at only about 60% of the expected depletion voltage.

A Microplex chip is mounted at each end of a detector and each chip reads out 128 alternate strips. The pulse height of the output signal from the Mi-

croplex chip for a given channel is proportional to the charge collected on the corresponding detector strip.

A detector assembly is shown in Fig. 1. The silicon detector, two Microplex readout chips, and printed circuit fanouts for the power, control, calibration, and output lines, are glued to a ceramic frame. This frame is in turn glued to a precision mount with the detecting strips parallel to its bottom edge. The three detector assemblies are then clamped together on a flat granite plate with the strips horizontal and with an equal inter-detector spacing of 2.1 cm.

3. The Test Beam and Data-taking

The telescope was exposed to a 15 GeV/c positron beam with a spot size of 0.9 mm FWHM, an angular divergence in the vertical direction of ± 0.3 mrad, and a beam spill of 100–200 nsec. The beam was adjusted to an average intensity of 0.1–0.5 particles/pulse at a rate of 10 pulses per second, and entered the telescope normal to the plane of the detectors. Upstream from the telescope was a scintillation counter S1. Downstream were two overlapping counters, S2 and S3, followed by a 10 radiation-length-deep lead glass shower counter.

The trigger for the data runs was a coincidence between a beam spill signal and the signals from S2 and S3. The effective gate width for registering particles in the silicon detectors was 500 nsec. For the background runs we triggered on a delayed beam spill signal. The 3×256 output signals from the telescope were multiplexed to a single BADC CAMAC module [8] which performed analog-to-digital conversion and first-order pedestal subtraction for each channel.

4. Data Analysis and Results

4.1 *Analysis*

The signal from each channel is corrected off-line for pedestal drift (evaluated about once per minute of data-taking), channel gain, and event-by-event baseline shift (due to noise common to all channels on a read-out chip or detector). A display of the corrected strip pulse height as a function of the strip number for the three detectors in a single event is shown in Fig. 2. The display clearly shows the trajectories of three particles, separated from each other by about 125 μm. The pulse height cut drawn at 42 BADC units (with 820 units = one volt) is used to define a hit as discussed below.

About 12% of the channels had low gains (identified by no response to the beam and/or noise levels below 10% of normal), or had large pedestal variations. These channels (and their immediate neighbors) have been excluded from the analysis. The problems associated with these channels are being investigated.

4.2 *Efficiency and noise rate*

We evaluate the detector efficiency as a function of the pulse height threshold. For this analysis, we restrict ourselves to events in which the lead glass counter and the scintillation counter S1 indicate that one and only one charged particle was present during the beam spill. We also require that two of the detectors have one and only one cluster (see below for the definition of a cluster), and that the track projection passes through the active region of the detector in question. Fig. 3 shows the probability of finding one or more strips in detector D with a pulse height above threshold as a function of that threshold. Using our out-of-time background runs, we also show the detector noise rate (defined as the probability of finding at least one strip in the detector above threshold) as a function of pulse height threshold. Taking a pulse height cut of 42, we find an efficiency of the active strips of $99.99 \pm 0.01\%$ (1 miss in 7300 events) and a

corresponding detector noise rate of $< 1.2 \times 10^{-3}$ (zero hits in 2000 background events).

Fig. 4 shows the differential strip noise distribution—a histogram for detector D of the pulse heights of all active strips in the background events. The Gaussian fit shown in the figure works remarkably well over more than four orders of magnitude. The fit gives $\sigma_{\text{noise}} = 8.1$. We observe no entries above the pulse height cut of 42; this allows us to set an upper limit on the noise rate of $< 8.4 \times 10^{-6}$ per strip per event.

4.3 *Clusters*

Now we look for "clusters" consisting of contiguous strips with significant pulse height. Our cluster algorithm is as follows: (1) we search for a strip with pulse height above 42 (about 5.2 σ_{noise}) to begin the cluster; (2) we add to the cluster any immediately adjacent strips with pulse height above 20 (about 2.5 σ_{noise}); and (3) we repeat step 2 until the adjacent strip pulse heights fall below the cut.

Fig. 5 shows the distribution of total cluster pulse height for detector D. The histogram is based on events in which the lead glass and S1 signals indicated the presence of a single particle, and for which one and only one cluster was found in each detector. The most probable pulse height is 136. Dividing this by the corresponding value of σ_{noise}, we find a signal-to-noise ratio of 17:1.

Fig. 6 shows the probability distribution for the number of strips per cluster. In Fig. 7 we show the average pulse height for the strip with the largest signal in the cluster, as well as the average pulse heights of the neighboring strips.

4.4 *Spatial resolution*

To evaluate the detector spatial resolutions, single particle events with a single cluster in each detector are analyzed. The spatial position y of a cluster is calculated by taking the pulse-height-weighted average coordinate of the strip with the largest signal and of the immediately adjacent strips which are included in the cluster. For the three equally spaced detectors we compute the residual r with $r = \sqrt{2/3}\ [y_2 - 1/2(y_1 + y_3)]$. Here, y_2 is the cluster coordinate for the center detector and y_1, y_3 are the coordinates for the two outer detectors. With this definition of r, the standard deviation σ_r will equal the spatial resolution σ_y, assuming that the three detectors have the same resolution. Fig. 8 shows three measurements of r with detector B, C, or D in the center. From Gaussian fits to these distributions, we obtain, respectively, the residual resolutions $\sigma_r(B) = 4.3 \pm 0.2\ \mu$m, $\sigma_r(C) = 4.8 \pm 0.1\ \mu$m, and $\sigma_r(D) = 3.9 \pm 0.2\ \mu$m. From these three quantities we can derive the individual detector resolutions, $\sigma_y(B) = 4.2 \pm 0.3\ \mu$m, $\sigma_y(C) = 5.2 \pm 0.1\ \mu$m, and $\sigma_y(D) = 3.4 \pm 0.3\ \mu$m. The contribution from multiple scattering is negligible.

4.5 *Two-particle separation*

Events containing two particles are selected by cuts on the lead glass and S1 signals. Using the same cluster algorithm as specified in Sect. 4.3, we look for the events with two clusters in each detector, compute the trajectories of the two tracks from the cluster positions, and plot in Fig. 9a a histogram of the separation of the tracks in the center detector. For normalization, we show in Fig. 9b the separation distribution for tracks taken from different events. The bin-by-bin ratio of histograms 9a to 9b is shown in Fig. 9c. Even with the very simple cluster algorithm we are now using, high efficiency for finding two tracks can be achieved for track separations greater than 150 μm. The residuals for the tracks found with separations less than 150 μm are plotted in Fig. 10; $\sigma_r(C) = 4.8 \pm 0.3\ \mu$m for these tracks indicating that there is no deterioration in the spatial resolution.

5. Conclusions

Silicon strip detectors equipped with Microplex readout chips can achieve:

- clean separation between signal and noise,
- a spatial resolution better than 5 μm, and
- two-track separation better than 150 μm with no deterioration in spatial resolution.

However, it is to be noted that these results are for detectors in a fixed-target configuration, with tracks at normal incidence. There remain many challenges ahead for successful operation at colliding beam machines such as the SLC, LEP, or the Tevatron Collider.

ACKNOWLEDGEMENTS

We would like to warmly acknowledge the help and support we have received from our colleagues at CERN, particularly Roland Horisberger, Leonardus Hubbeling, Bernard Hyams, and Peter Weilhammer. The original design of the VLSI circuit was by J. T. Walker. Chris Kendrick of the Center for Integrated Systems, Stanford University, provided valuable help in its initial testing.

REFERENCES

1. For example, see R. Bailey *et al.Nucl. Instr. and Meth.* **226** (1984) 56.
2. Silicon microstrip vertex detectors have been proposed for the Delphi and Aleph experiments at LEP, the CDF experiment at the Tevatron Collider, and the Mark II experiment at the SLC.
3. Details can be found in the "Proposal for the Addition of a Silicon μ-strip Detector to the Mark II Detector at the SLC", by the Mark II Collaboration, SLAC Proposal, September, 1985 (unpublished).
4. J. T. Walker *et al.Nucl. Instr. and Meth.* **226** (1984) 200.
5. G. Anzivino *et al.Nucl. Instr. and Meth.* **A243** (1986) 153.
6. C. Adolphsen *et al.IEEE Trans. Nucl. Sci.* **NS-33** (1986) 57.
7. These are prototype detectors fabricated by Micron Semiconductor, Ltd., Lancing, Sussex, U.K.
8. M. Breidenbach *et al.IEEE Trans. Nucl. Sci.* **NS-25** (1978) 706.

Table 1

Detector Property	Detector B	Detector C	Detector D	Units
Pitch	25	25	25	μm
Active Length	60	60	60	mm
Active Width	6.4	4.6	6.4	mm
Thickness	285	292	315	μm
Guard Ring	no	yes	yes	
Implant Width	17	10	10	μm
Interstrip Capacitance*	11	8	8	pF
Depletion Voltage	$\approx$55	$\approx$55†	$\approx$55	V
Operating Voltage	55	32	55	V
# of Bonded Channels	256	185	256	
Fraction of Working Channels	91	95	79	%

* calculated

† expected

Figures

1. Photograph of a detector assembly.
2. A display of the corrected strip pulse height vs. the strip number for the three detectors in a single event. The dashed line indicates the pulse height threshold cut for a hit. The problem channels (and their immediate neighbors) which have been excluded from the analysis are set to zero pulse height in this plot.
3. The probability of finding one or more strips in detector D with a pulse height above threshold as a function of the threshold. Results for both data runs and background runs are shown.
4. The differential strip noise distribution for detector D. The curve represents a Gaussian fit with $\sigma = 8.1$ BADC units.
5. The cluster pulse height distribution for detector D.
6. The probability distribution for the number of strips per cluster in detector D.
7. The average pulse heights for the strips in a cluster as a function of the relative strip number. The strip with the largest signal is given a relative strip number of zero. The data are for detector D.
8. (a)–(c) The histograms of the residuals (defined in the text) for data runs in which, respectively, detector B, C, or D was the center detector. The fits shown are Gaussian.
9. (*a*) Histogram of the calculated separation of tracks in two-track events.

   (*b*) Histogram of a simulated two-track separation using tracks from different events.

   (*c*) Ratio of (a) to (b), calculated on a bin-by-bin basis. The dashed line indicates the average ratio for two-track separations between 200 and 500 μm.

10. A histogram of the residuals for all tracks found in the two-track events with separation < 150 μm. The fit is a Gaussian.

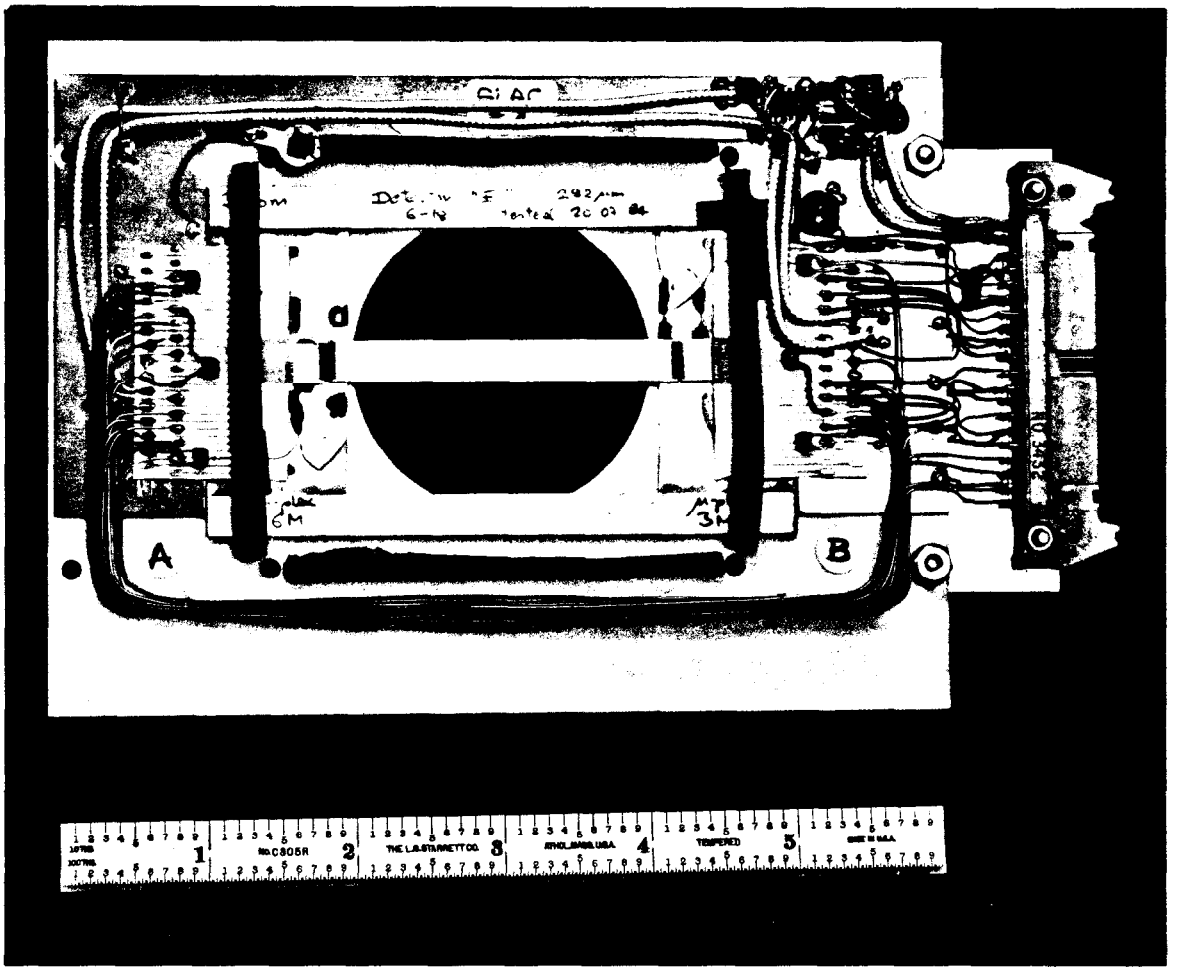

Fig. 1

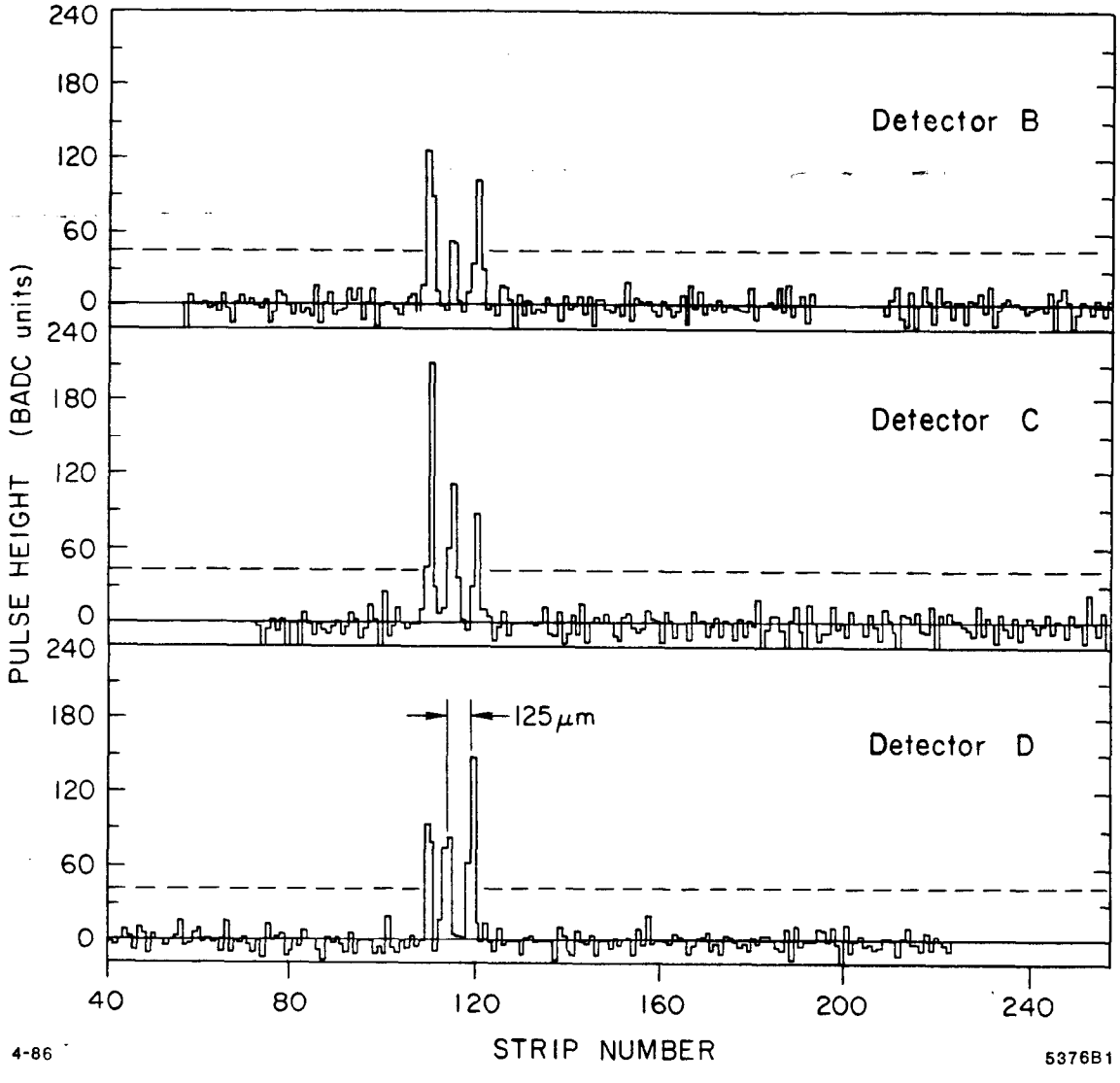
240
180
120
60
0
Detector B
240
180
120
60
0
Detector C
240
180
120
60
0
125 μm
Detector D
PULSE HEIGHT (BADC units)
40
80
120
160
200
240
STRIP NUMBER
4-86
5376B1

Fig. 2

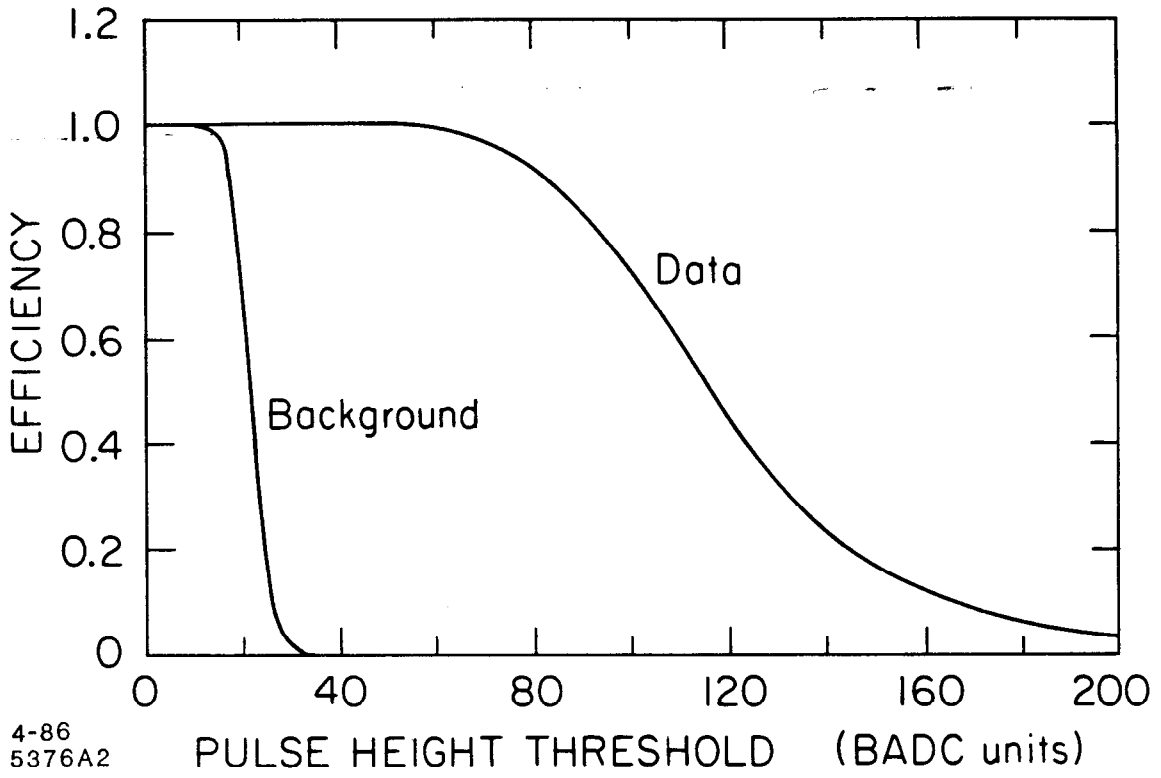
1.2
1.0
0.8
0.6
0.4
0.2
0
EFFICIENCY
Data
Background
0
40
80
120
160
200
4-86
5376A2
PULSE HEIGHT THRESHOLD (BADC units)

Fig. 3

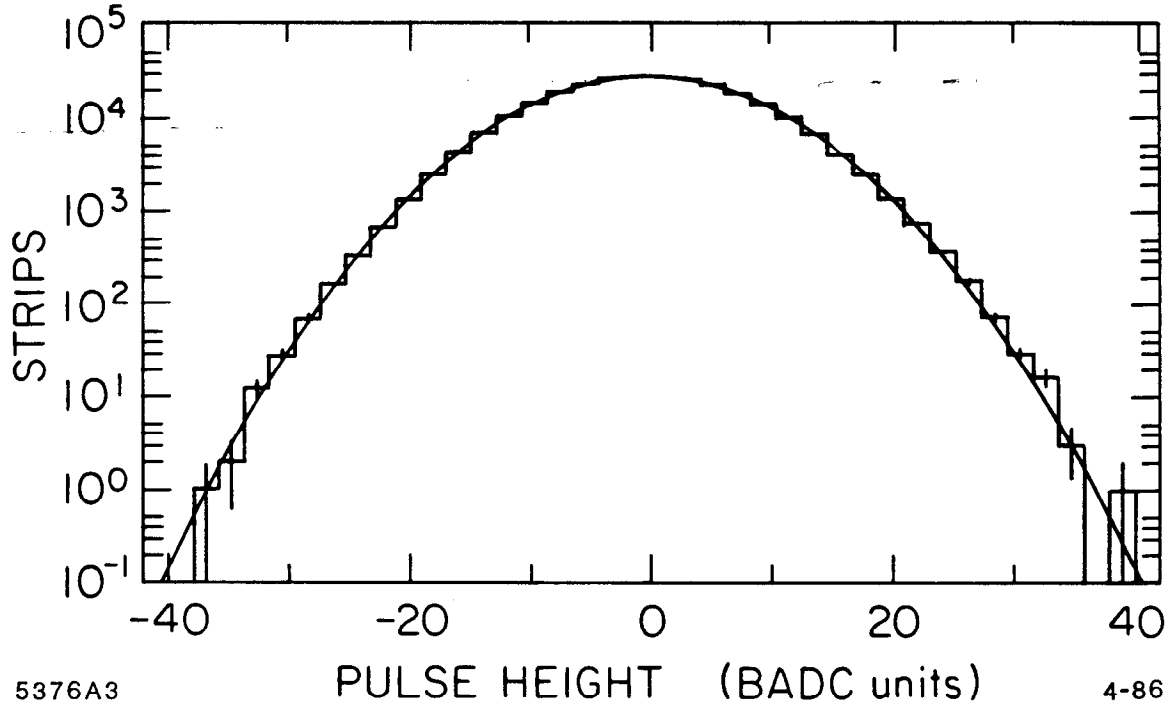
STRIPS
10^5
10^4
10^3
10^2
10^1
10^0
10^{-1}
-40
-20
0
20
40
PULSE HEIGHT (BADC units)
5376A3
4-86

Fig. 4

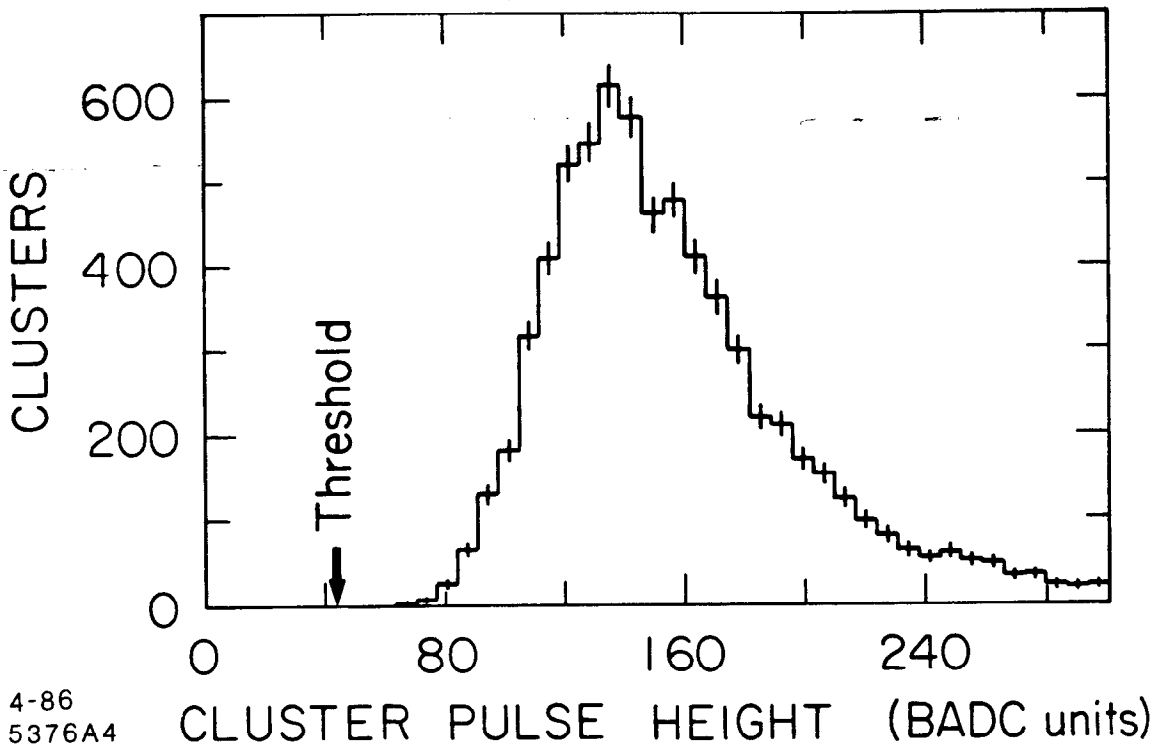
600
400
200
0
CLUSTERS
Threshold
0
80
160
240
4-86
5376A4
CLUSTER PULSE HEIGHT (BADC units)

Fig. 5

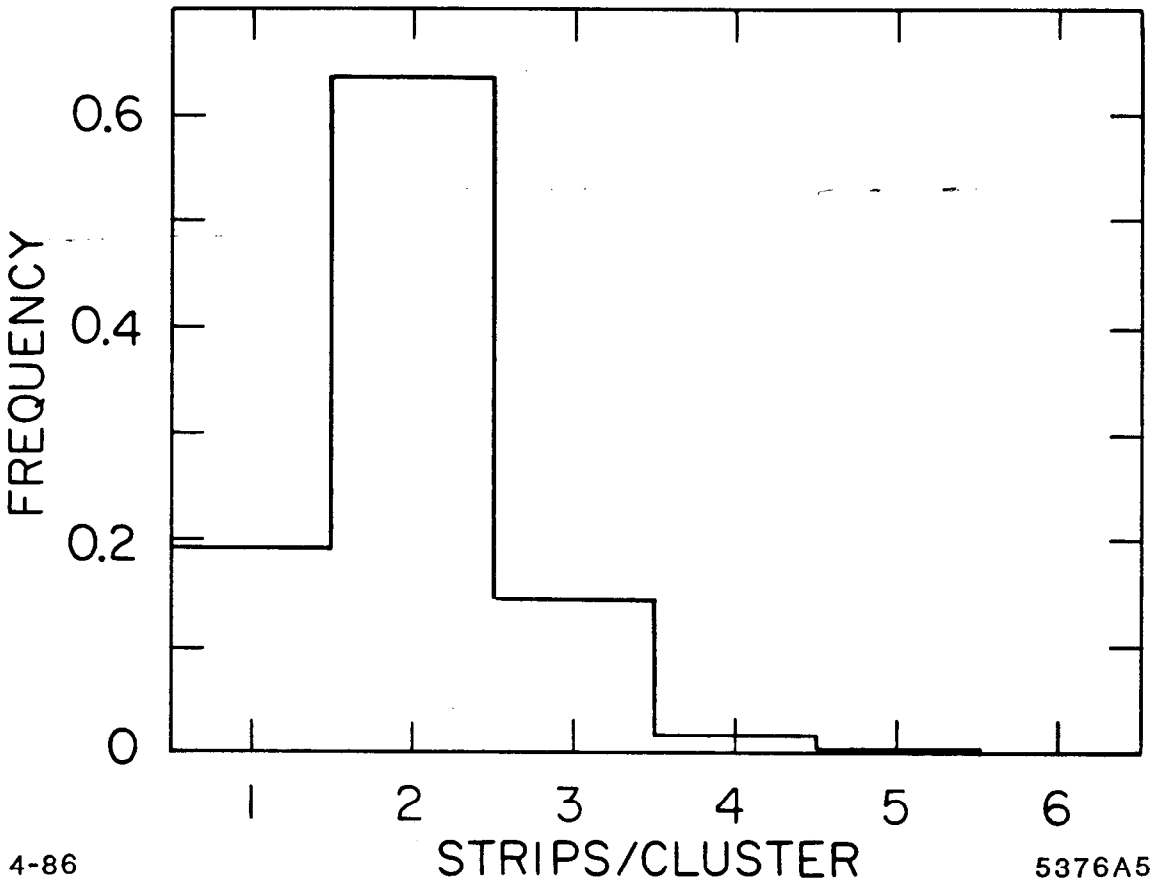

Fig. 6

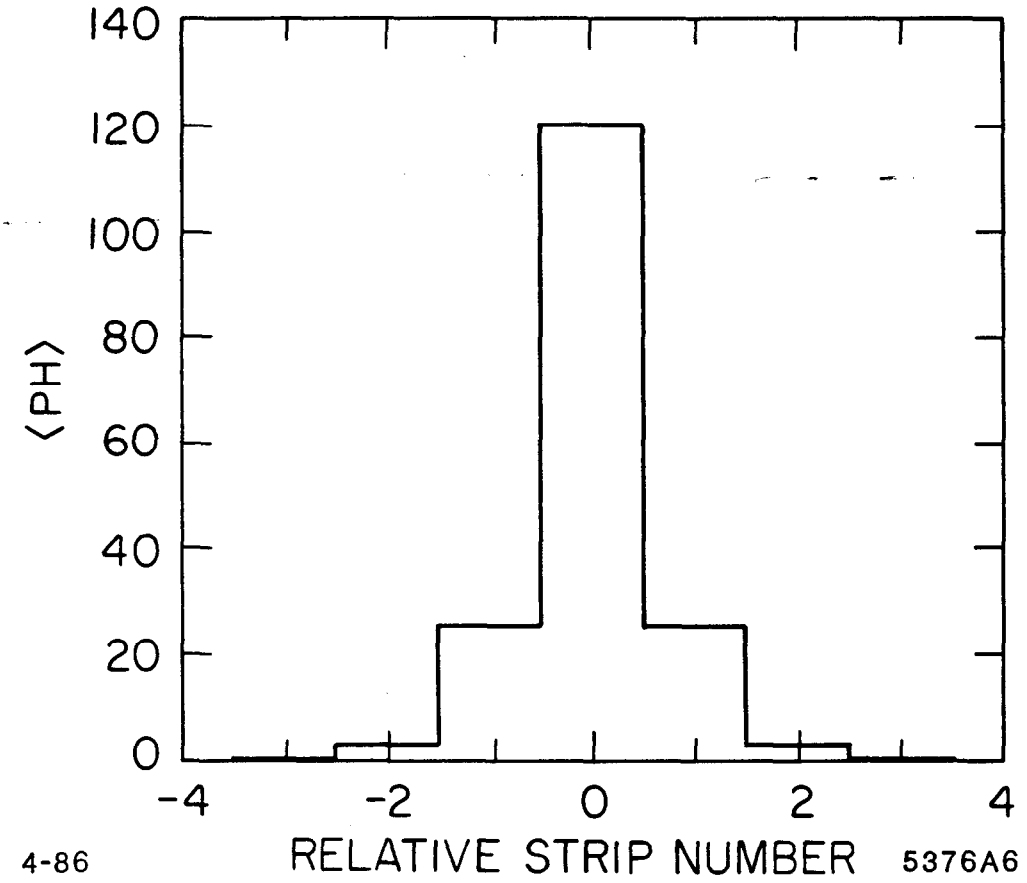
140
120
100
80
60
40
20
0
<PH>
-4
-2
0
2
4
RELATIVE STRIP NUMBER
4-86
5376A6

Fig. 7

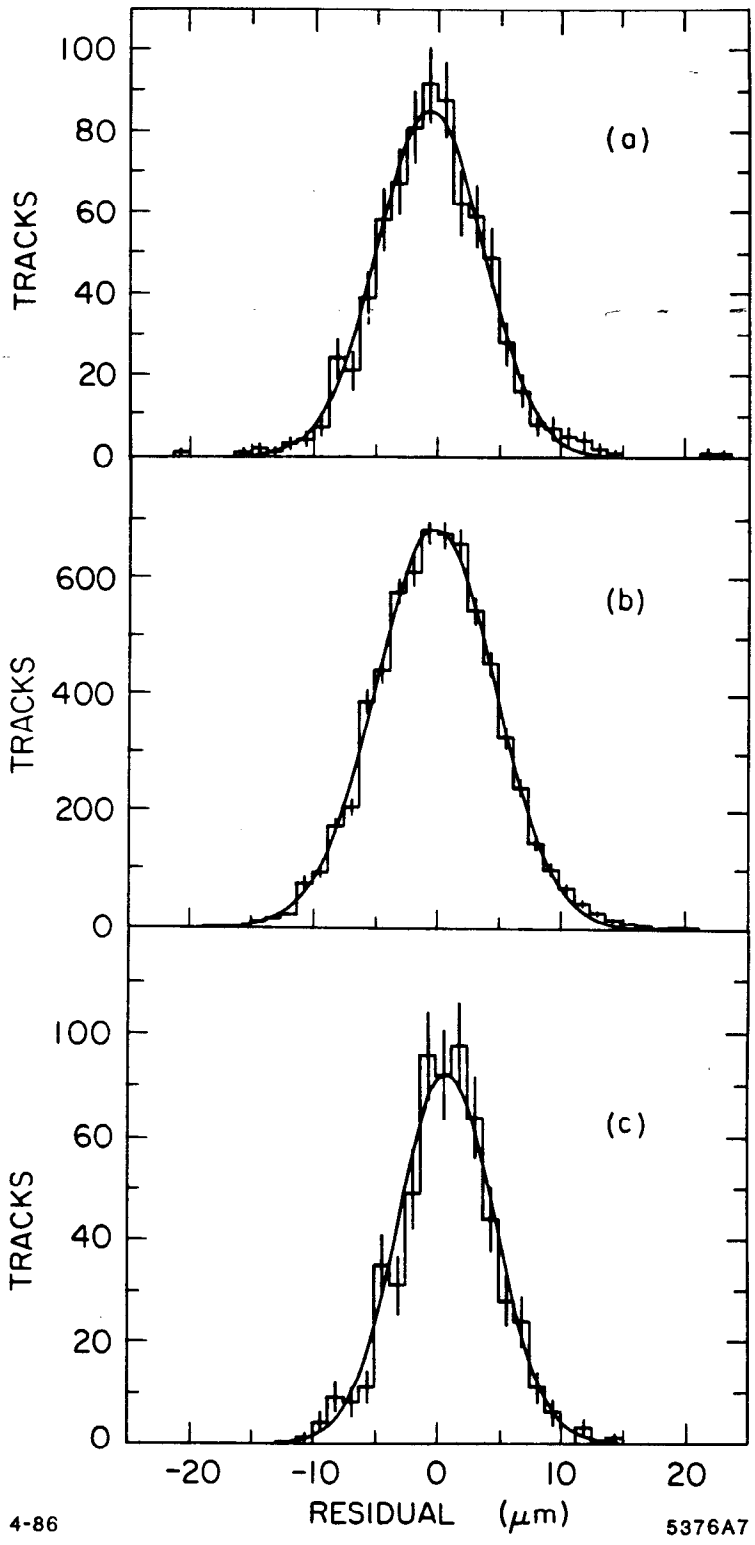
100
80
60
40
20
0
TRACKS
(a)
600
400
200
0
TRACKS
(b)
100
60
40
20
0
TRACKS
(c)
-20
-10
0
10
20
RESIDUAL (μm)
4-86
5376A7

Fig. 8

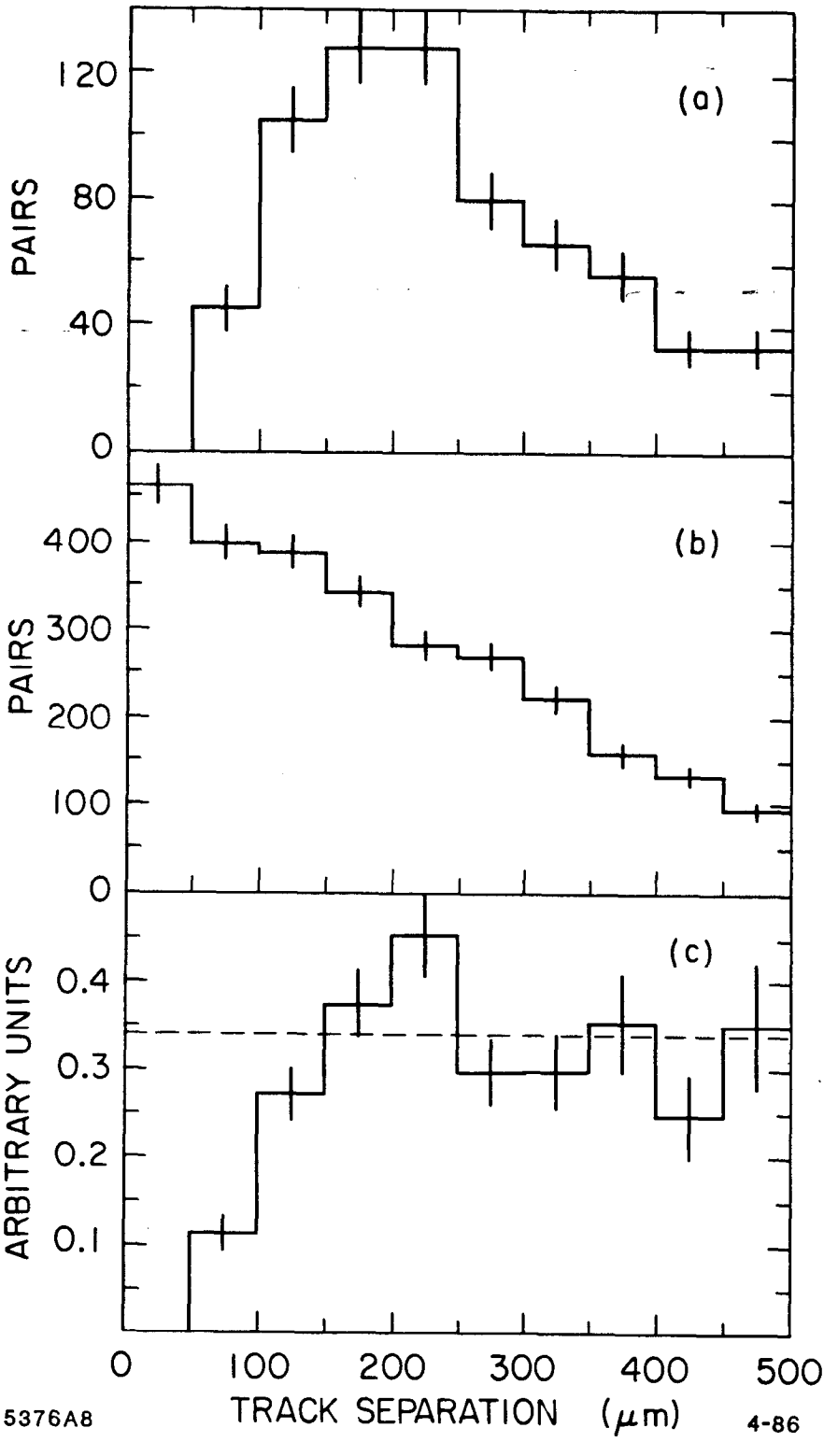
120
80
40
0
PAIRS
(a)
400
300
200
100
0
PAIRS
(b)
0.4
0.3
0.2
0.1
ARBITRARY UNITS
(c)
0
100
200
300
400
500
TRACK SEPARATION (μm)
5376A8
4-86

Fig. 9

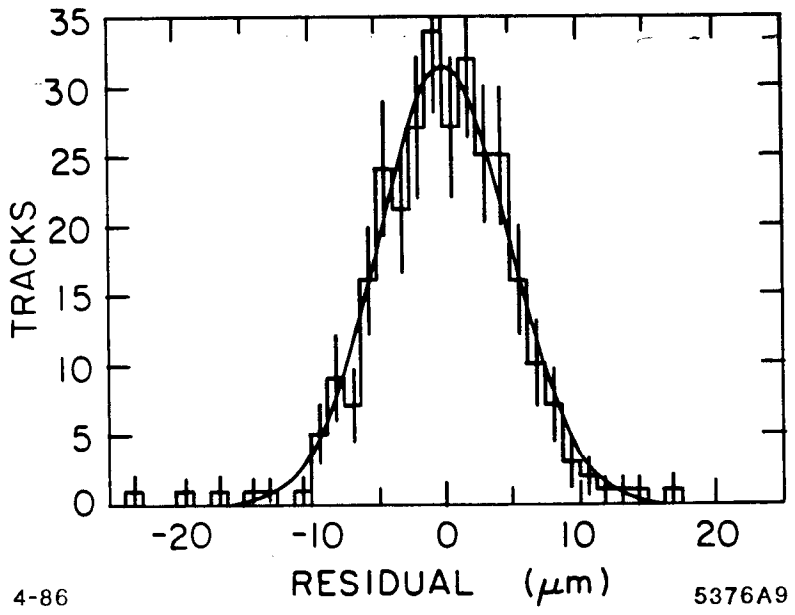

Fig. 10